

Cite this: *Lab Chip*, 2012, **12**, 1289

www.rsc.org/loc

PAPER

Array-based capture, distribution, counting and multiplexed assaying of beads on a centrifugal microfluidic platform[†]

Robert Burger,* Patrick Reith, Gregor Kijanka, Victor Akujobi, Patrick Abgrall and Jens Ducré*[†]

Received 28th November 2011, Accepted 3rd February 2012

DOI: 10.1039/c2lc21170j

We present a novel centrifugal microfluidic platform for the highly efficient manipulation and analysis of particles for applications in bead-based assays. The platform uses an array of geometrical V-cup barriers to trap particles using stopped-flow sedimentation under highly reproducible hydrodynamic conditions. The impact parameters governing the occupancy distribution and capture efficiency of the arrayed traps are investigated. The unique, nearly 100% capture efficiency paired with the capability to establish sharply peaked, single occupancy distributions enables a novel, digital readout mode for color-multiplexed, particle-based assays with low-complexity instrumentation. The presented technology marks an essential step towards a versatile platform for the integration of bead- and cell-based biological assays.

Introduction

Microfluidic systems offer a manifold of advantages such as short diffusion times and precise control of (laminar) flow and shear rate and therefore have the potential to leverage innovative tools for biological assays and drug discovery.¹ Typical applications are cell- and bead-based assays where it is mandatory to capture particles in a well-defined manner and expose them to a variety of conditions.^{2,3} In bead-based assays, specific capture probes are immobilized on the surface of beads which are typically labeled by a unique spectroscopic fingerprint or distinguished by the fluorescent tag of a detection antibody. Using conventional instruments, the handling of the suspended beads in the assay protocol is rather straightforward. However, the spectroscopic identification of the beads and the (simultaneous) readout of the assay signal originating from their surface constitute major microfluidic, optical and instrumental challenges. In most cases a complex and expensive apparatus akin to commercial flow cytometry systems is required for detection.

Further issues arise from the miniaturization of bead-based assays. In macroscopic systems, homogeneous assay conditions can be assured by stirring, and reagents can be readily exchanged by using filters or magnetic beads. In miniaturized systems, micro particles can be captured using for example hydrodynamic trapping in meander channels.^{4,5} Furthermore, beads can be embedded in a matrix of a support material⁶ or they can be aggregated, *e.g.* in step- or weir-structures,^{7,8} and then exposed to a sequence of reagents in flow-based schemes. Such bead

aggregates are very difficult to control in three dimensional microcavities and also lead to a high fluidic resistance. They are commonly prone to display statistical voids and noticeable fractions of the layers may even be missing, in particular at the ceiling of microfluidic channels. Due to the interplay of the laminar flow conditions prevailing in microstructures, the parabolic Poiseuille flow profile and the commonly rather wide pore size distribution in the bead aggregate, a considerable spread between the individual assay conditions for each bead is thus very common. This intrinsic lack of hydrodynamic control severely affects the biochemical assays, *e.g.* through the total amount of sample passing across the surface of beads, the binding kinetics and the efficiency of washing due to uncontrollable, local variations of fluid shear.

In the overall context of (multiplexed) bead- and also cell-based assays, this paper introduces a novel strategy for the capture, retention and treatment of particles which will also facilitate a digital mode for counting and ID of the particle content in a given aliquot. Several methods for bead or cell trapping have been reported in the past. Common methods are dielectrophoretic trapping (DEP) and hydrodynamic trapping. Yang *et al.*⁹ showed a setup comprising of two parallel channels separated by a dam structure where cells were trapped due to the flow between the two channels. Di Carlo *et al.*¹⁰ presented an array of capture elements using a pressure driven flow. These capture elements were designed to leave a 2-μm gap in the vicinity of the eventual capture location to promote liquid flow through the capturing elements. Skelley *et al.* advanced this approach to retain two different cells in each capturing site for cell pairing.¹¹ A similar technique was also used by Khoury *et al.* for on-chip culturing of human stem cells.¹² Kim and coworkers recently published a chip for trapping bacteria from a pressure driven flow.¹³ Gravity driven sedimentation approaches to capture cells

Biomedical Diagnostics Institute, National Centre for Sensor Research, School of Physical Sciences, Dublin City University, Glasnevin, Dublin 9, Ireland. E-mail: robert.burger2@mail.dcu.ie; jens.ducree@dcu.ie

† Electronic supplementary information (ESI) available. See DOI: 10.1039/c2lc21170j

in microwells have also been investigated in the past.^{14,15} Lee *et al.* developed a system using the artificial gravity created in a centrifugal microfluidic system to trap cells.¹⁶ In their system, a cell suspension was flown through a radially sloped channel with pockets in the side walls where the cells were trapped under the impact of the centrifugal force. Martinez-Duarte *et al.* showed a DEP filter integrated on a centrifugal microfluidic platform, using carbon electrodes to filter cells.¹⁷ Another centrifugal microfluidic structure using DEP for cell separation was presented by Boettcher *et al.*¹⁸

Centrifugal microfluidic systems offer unique solutions for sample preparation and liquid handling. Various functions such as valving, metering, mixing, diluting and particle separation have been shown in the past.^{19–21} Furthermore, this technology enables development of low cost point of care devices.²²

In our novel scheme, suspended particles such as 20-μm polymer beads are captured in an array of V-cups under stopped-flow conditions, *i.e.* by mere sedimentation, during fast rotation of the disc-shaped substrate. Compared to typical, flow-driven capture schemes, our new method utilizes microfluidic structures which are easier to manufacture (*e.g.* no vertical gaps are necessary to promote flow through the cups), does not need to connect to periphery such as external pumps, and offers an unprecedented level of capture efficiency. Furthermore, the scheme presented here with beads is also applicable to cells. The influence of the ratio between the particle size and the active capturing zone of the V-cups on the particle occupancy per cup and the overall capture efficiency are investigated. We found that the particle count distributions can be tuned to a sharp peak at a single occupancy per V-cup. Such single occupancy distributions introduce highly homogeneous and reproducible assay conditions for bead- and cell-based assays. This novel particle capture scheme is the most critical element towards a comprehensive platform for capturing and analyzing beads and cell populations on a centrifugal platform.

Experimental method & materials

Device fabrication

All devices used in this work have been fabricated in PDMS (Sylgard 184, Dow Corning GmbH, GERMANY). Molds for PDMS casting are surface micromachined using a combination of SU8-3025 (Microchem, USA) for manufacturing the V-cup array and dry film resist (WBR 2100, DuPont, USA) for the reservoirs. To this end, a 30-μm layer of SU-8 is spin-coated onto a 4" silicon wafer and baked on a level hot plate at 95 °C for 14 min. Subsequently, the wafer is exposed to UV light (exposure energy 280 mJ cm⁻²) using a mask aligner (MA56, Süss MicroTec, GERMANY). To minimize the taper angle of the side walls, wavelengths below 350 nm have been suppressed using a long pass filter (PL-360-LP, Omega Optical, USA). Post exposure bake (PEB) has been performed at 95 °C for 3 min. Next, the SU-8 has been developed using standard developing solution and hard baked for 1 min at 150 °C. In a second step two layers of dry resist are laminated on top of the SU-8 at a roll temperature of 95 °C to create a layer with a total thickness of 200 μm. In the following step, the dry film is exposed to UV light (energy density of 440 mJ cm⁻²). After exposure the wafer is baked on a hot plate

at 100 °C for 1 min. Unexposed resist is removed in a bath of 1.6% K₂CO₃. To avoid sticking of PDMS to the mold, the wafer has been coated by immersing it for 2 h in Hexane (Sigma Aldrich, IRELAND) with 10 mM Octadecyltrichlorosilane (Sigma Aldrich, IRELAND), rinsed with Methanol and baked at 100 °C on a hotplate for 1 h, thus creating a hydrophobic anti-sticking coating.

To replicate this template, PDMS was mixed in ratio of 5 : 1 (base to curing agent by weight), poured on the mold and degassed under vacuum for 20 min. The PDMS was then partially cured in the oven at 85 °C for 15 min and removed from the mold. Access holes have been punched into the PDMS slab. The disc was sealed with a blank PMMA disc exhibiting a spin coated layer of PDMS in a ratio 20 : 1 (base to curing agent by weight) on its surface which has been cured in the oven for 20 min. The PMMA-PDMS assembly was eventually baked at 85 °C for 3 h to establish irreversible bonding.²³ Fig. 1 shows one of the discs used in this work.

Preparation of microfluidic chip

The microfluidic structures used in this work contain arrays with a density of capturing elements ranging between 180 and 340 elements per mm², depending on the size of the V-cups. Each chamber contains 1350–3500 single capture elements. To assure complete and bubble-free filling, the device is placed in a vacuum prior to introducing the liquids.²⁴ A computer controlled motor (Faulhaber Minimotor SA, SWITZERLAND) sets the spin rate of the disc. Imaging during rotation was achieved using a highly sensitive camera (Sensicam QE, PCO, GERMANY) attached to a motorized 12x zoom lens (Navitar, USA) in a setup similar to the one presented by Grumann *et al.*²⁵

Working principle

The system presented in this work is based on the sedimentation of particles in a suspending medium due to the influence of the centrifugal force and subsequent mechanical trapping of the particles in an array of mechanical traps. The array comprises

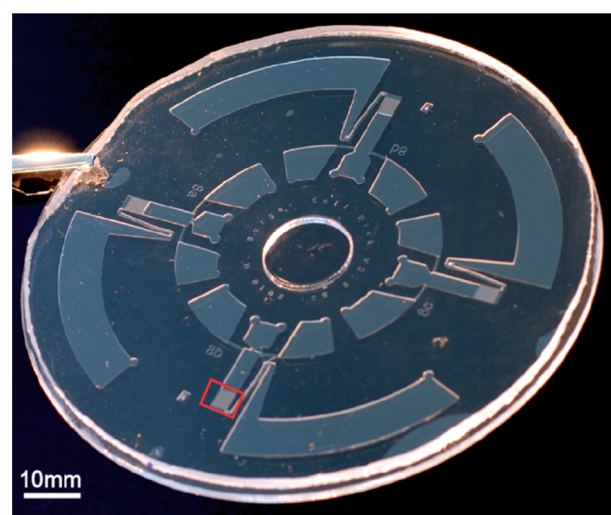


Fig. 1 PDMS disc with four identical fluidic structures used in this work. The position of one capturing array is marked by the red square.

of a staggered arrangement of v-shaped cups with each subsequent line shifted by $1/3$ of the center-to-center distance λ between two neighboring cups. This arrangement eliminates free radial pathways between the sample inlet and the bottom of the chamber. Initially, the array is completely filled with pure liquid.

Beads are then introduced radially inwards from the cup array. Rotating the disc induces a radially directed sedimentation of the beads which are denser than the surrounding liquid. The capturing chamber is designed such that there is no flow of liquid during the capturing process, *i.e.* capturing is performed under stagnant flow conditions. When a bead sedimenting into the array hits a cup sufficiently close to its center, the bead becomes mechanically trapped. The capturing and medium exchange process is shown in Fig. 2 and 3, respectively to illustrate the working principle.

The size of the cups determines the number of beads it can hold and hence the occupancy can be adjusted ranging from single to multi-bead occupancy depending on the ratio $R_c = d_c/d_B$ of the active capturing cross section of the cups d_c and the diameter of the beads d_B .

Since the particles sediment in a stagnant liquid, our new method overcomes a major drawback of pressure driven capturing schemes. This drawback is linked to the continuity of streamlines which diverge around obstacles and hence drag the particles around the capturing elements. This effect has previously been suppressed in part by introducing small gaps in the capture elements, *e.g.* slits or vertical gaps between the top of the

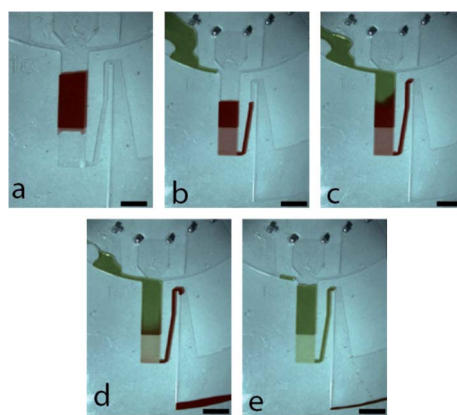


Fig. 3 Medium exchange in v-cup chamber. The chamber is completely filled with a first liquid (red) (a). The disc is then stopped and a second liquid (green) is introduced (b). Subsequent spinning of the disc transfers the second liquid into the array chamber where the first liquid is completely replaced (c–d). Scale bars are 1 mm.

trapping structures and the lid.^{10,12,13} These sieve-like openings are too narrow for the particles to pass, but they do add flow components directed through the center of the capturing elements.

However, in particular for small, micron-scale beads, these structures are rather complex to manufacture and tend to result in only a slight improvement of the capture efficiency. In recent experiments on pressure driven cell capturing, Kim *et al.*

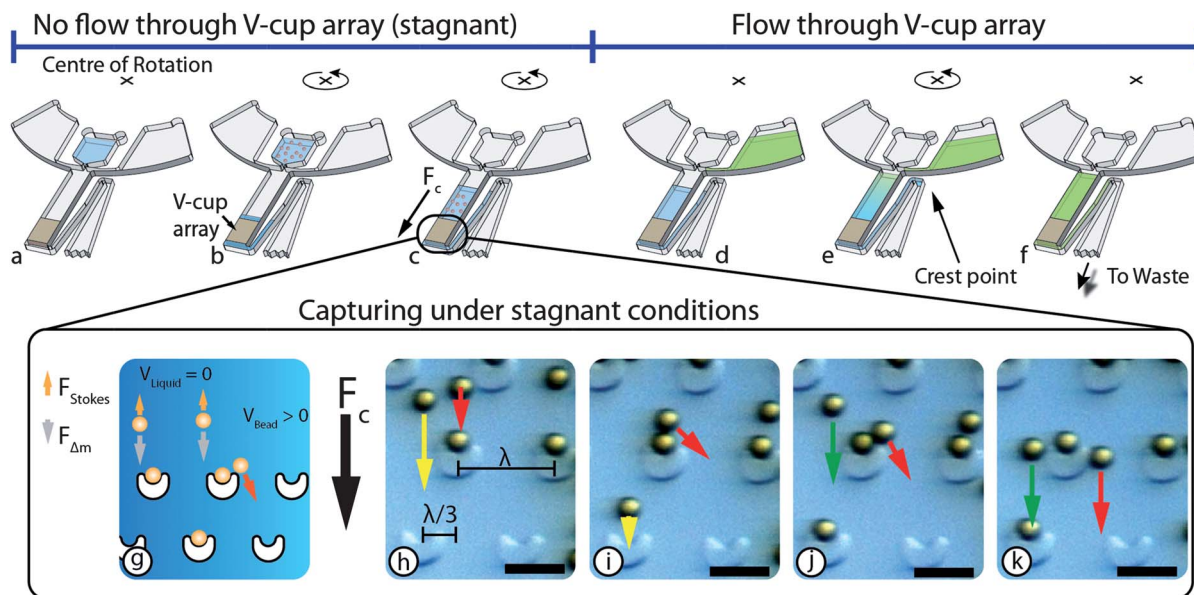


Fig. 2 Bead capturing and procedure for medium exchange. (a) Introduction of a small volume of liquid to fill the capturing array and to enable particle sedimentation. (b) Particle suspension is filled in the central reservoir and the disc is spun, resulting in a transfer of the particle suspension on top of the liquid in the capturing array and the sedimentation of the beads (b, c) (until this point there is no flow of liquid through the array). The medium in the bead capturing chamber can be displaced by introducing a second liquid in the reservoir and spinning the disc. The liquid flows into the capturing chamber, resulting in the rise of the liquid level above the crest point of the siphon. This leads to a liquid flow into the waste reservoir (d, e). If the volume of the second liquid is larger than the volume of the capturing chamber, the liquid volume in the chamber is exchanged (f). This can be repeated successively in order to expose the particles to different reagents. Image g illustrates the capturing principle and forces acting on the beads while the sequence h–k shows the capturing of 20- μm PS beads in an array of cups with $R_c = 1$. The yellow arrow shows the capturing of a bead in a cup while the red and green arrows show the sedimentation and deflection of beads along their approach of already occupied cups. A video of the capturing process is also available as supplementary information. Scale bars are 50 μm .

reported maximum capture efficiencies of particles as low as 1%,¹³ whereas our system can be readily configured to achieve a theoretical capture efficiency of 100%. Our experimental results come indeed very close to the theoretical limit.

To enable washing, treatment and staining of the captured particles, the medium in the V-cup chamber is exchanged *via* a siphon-based mechanism. The radial position of the crest point of the siphon sets the maximum filling level of the V-cup chamber. So adding an amount of liquid corresponding to the dead volume of the array chamber will prime the siphon past its crest point and completely replace the original medium surrounding the beads under the prevalent laminar flow conditions in our microfluidic system. While keeping the flow rates during the exchange sufficiently low, the vast majority of beads remain trapped.

Bead-based immunoassays

The particle suspensions used for the immunoassays consisted of 20- μm polystyrene beads (Microparticles GmbH, GERMANY) diluted in PBS with 5% Bovine Serum Albumin (BSA) (Sigma-Aldrich, IRELAND) to reduce agglomeration and sticking to the PDMS. All immunoassay experiments have been carried out using three colors of 20- μm polystyrene beads. Each color corresponds to a different IgG coating: mouse anti-ER α IgG (sc-8002, Santa Cruz, USA) (white PS beads), human IgG (MS143, Biomeda corp., USA) (red PS beads) and rabbit Anti-fd Bacteriophage IgG (B2661, Sigma-Aldrich, IRELAND) (blue PS beads). The analyte for the immunoassay contained goat-anti-mouse antibodies (Ab, IgG1) labelled with Alexa Fluor 488 (A11001, Invitrogen, USA), goat anti-human Ab (IgG2) labelled with Alexa Fluor 488 (A11013, Invitrogen, USA) and goat anti-rabbit Ab (IgG3) labelled with Atto 488 (A11008, Invitrogen, USA).

For the bead-based immunoassays capture array comprising of cups with an active capture zone diameter of 20 μm have been used in order to induce distributions which are sharply peaked at single bead occupancy. In a first step, the array region has been filled with 2 μl of PBS buffer with 5% BSA. Next 2 μl of bead suspension (\sim 2000 beads μl^{-1}) has been filled in the bead reservoir. The disc was immediately spun at 20 Hz in order to transfer the bead suspension in the array chamber and capture the beads in the V-cups. Shake mode capturing was applied to achieve single bead occupancy per cup. After the capturing step, the disc was stopped and 8 μl of analyte (containing IgG1, IgG2 or IgG3) was pipetted into the sample reservoir. The disc was then rotated again at 20 Hz, leading to a flow of the analyte into the array chamber accompanied by the displacement of the initial liquid through the siphon channel into the waste chamber. After the full substitution of the first liquid, the disc is stopped and incubated at room temperature for 90 min.

Following the incubation step, the array is washed 3 times with 8 μl PBS buffer containing 0.1% BSA to remove all unbound antibodies. Subsequently, the fluorescence of the beads is measured using an inverted fluorescence microscope (IX 81, Olympus, Japan) with a FITC-compatible filter.

Results and discussion

Characterization of particle capture

To characterize the influence of the ratio of the active capturing cross-section of the V-cups to the bead diameter on the occupancy distribution of the trapped beads, discs with three different cup sizes ($d_c = 14 \mu\text{m}$, 20 μm and 32 μm) were prepared and tested with 10 μm and 20 μm diameter particles, respectively. We observed that the spinning frequency does not have a decisive impact on the capture efficiency, but only on the time required for the sedimentation of the particles. Therefore, all subsequent experiments were run at the same rotational frequency of 20 Hz. It was also observed that a “shake mode” step was advantageous to narrow the occupancy distribution. To this end the following spinning protocol has been used:

1. Bead capturing at 20 Hz
2. Shake mode (acceleration 75 Hz s^{-1} , 40 Hz for 10 s, deceleration 75 Hz s^{-1} , 2 Hz for 10 s, 30 cycles)

The results for 10- μm silica bead experiments show that for a ratio $R_c = 1.4$, 94% of all occupied cups contain a single bead, while only 0.8% of all cups remained empty. Increasing R_c to 2 leads to a broader occupancy distribution characterized by 57% and 26.6% of single and double occupancy, respectively, and only 2.7% of all cups are left empty. It is to be noted that in particular the number of empty cups also depends on the absolute number of introduced beads. Moving R_c further up to 3.2 shifts the maximum of the significantly broadened occupancy distribution to 8 beads per cup. For $R_c = 1$, 99.5% of all occupied cups contain a single bead. Increasing R_c to 1.6 leads to a wider distribution where 48.8% are occupied by one bead, 27.7% contain 2 beads and 11% contain 3 beads. The results are shown in Fig. 4.

These results demonstrate that it is possible to influence the number of trapped beads per cup by adjusting the ratio between particle diameter and capturing area of the cups. While the occupancy distribution for increasing R_c widens, the distribution shows a sharp peak for R_c values of 1 and 1.4 with > 94% single occupancy. This demonstrates that a high percentage of single occupancy can be achieved, even if R_c varies. This is important considering that biological cells are polydisperse, *i.e.* a population exhibits a wider size distribution. Capturing single particles in well-defined locations is an important capability to enable single-cell or bead-based assays as well as particle counting.

Particle capture efficiency

The particle capture efficiency was assessed using 20- μm PS beads and cups with $R_c = 1$ to establish a sharp, single-occupancy distribution. Suspensions with various bead concentrations were then introduced into the disc and captured using the following protocol:

1. Spinning at 20 Hz for 4 s - clockwise
2. Spinning at 20 Hz for 1 s - counterclockwise
3. Shake mode

The capture efficiency was then determined using the following methodology: the total number of all beads (b_T) entering the array was counted in each experiment. Additionally the amount of captured (b_C) and by-passing (b_B) beads was counted. The

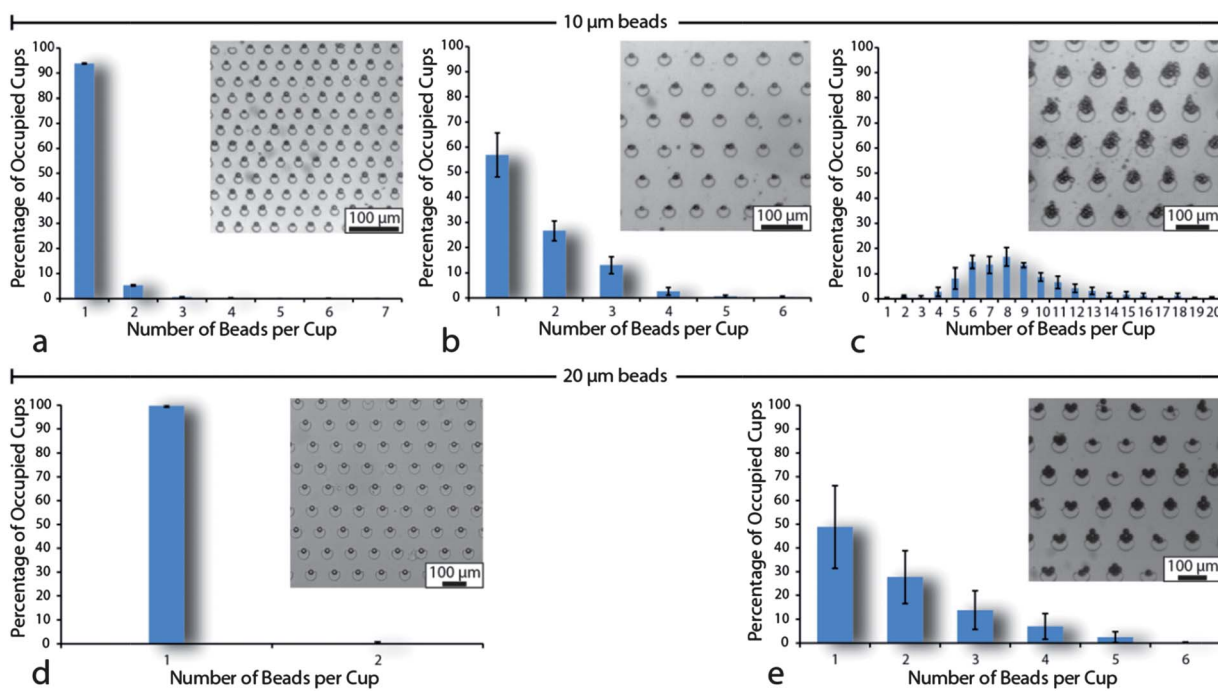


Fig. 4 Occupancy distribution for different cup sizes with 10-μm silica beads (a–c) and 20-μm PS beads (d and e). a) Capture elements with a 14-μm active capturing area. 94% of all occupied cups contain a single bead. Only 0.8% of all cups remained empty. b) Increasing the active capturing area to 20 μm leads to a broader occupancy distribution, and only 2.7% of all cups stayed empty. c) Occupancy distribution for cups with a 32-μm capturing area. The maximum of the distribution shifted to 8 beads per cup, leaving 0.9% of all cups empty. d) $R_C = 1$, 99.7% single occupancy and only 5% of all cups empty. e) $R_C = 1.6$, 48.8% are occupied by a single bead and 27% contain 2 beads. Insets show typical bead distributions in the capture array.

term by-passing beads describes beads which travel along the side wall of the capturing chamber and cannot be captured due to the absence of V-cups at the side wall.

Introducing cups on the side wall would result in agglomerates of beads in their vicinity. Typically, 3–5% of all beads entering the array bypassed the cups. For applications where high capture efficiency is of paramount importance, bypassing beads could be largely eliminated by increasing the width of the capture array.

The capture efficiency was then calculated using the following formula:

$$\text{Capture efficiency} = b_c / (b_T - b_B)$$

Additionally the array occupancy was also calculated:

$$\text{Array occupancy} = b_c / n_c$$

Whereas n_c is the total number of cups in the array. For all capture efficiency experiments n_c amounts to 1358.

These results show the very high capture efficiency of the stagnant flow scheme. For low bead concentrations, *i.e.* a ratio of beads to cups (R_{bc}) $\ll 1$, the capture efficiency is close to 100% and even for a ratio of 0.78 the capture efficiency is still above 90%. For $R_{bc} = 0.95$, 86.9% of all beads are captured and 83% of the array are occupied (Fig. 5). The fact that the capture efficiency is high for a low bead-to-cup ratio but decreases when the ratio approaches unity underlines the importance of a homogeneous bead distribution over the whole extent of the array. This is necessary to assure that all beads are trapped because they always encounter an unoccupied cup before leaving the array.

With the here presented setup, a R_{bc} of 0.46 results in a capture efficiency of 99.1% which demonstrates the feasibility of performing a full particle count with high accuracy. Methods to improve the particle distribution are currently investigated since increasing R_{bc} while at the same time maintaining a high capture efficiency would allow to reduce the footprint of the array.

Multiplexed, bead-based immunoassay

Due to the intrinsic advantages of the sedimentation-based V-cup array technology such as highly reproducible hydrodynamic conditions and the arrayed presentation of beads in

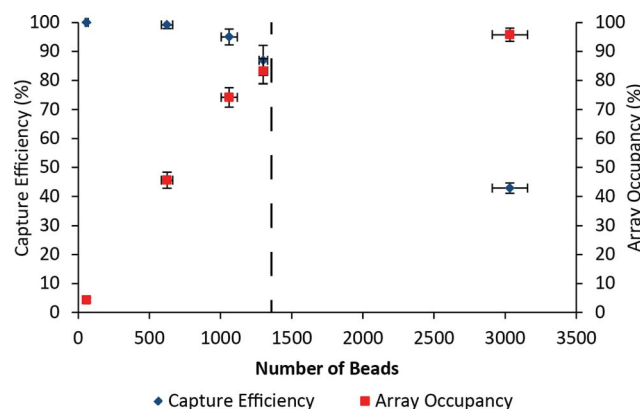


Fig. 5 Bead capture efficiency and array occupancy depending on the amount of beads presented to the array. The dashed line indicates the total number of cups in the array.

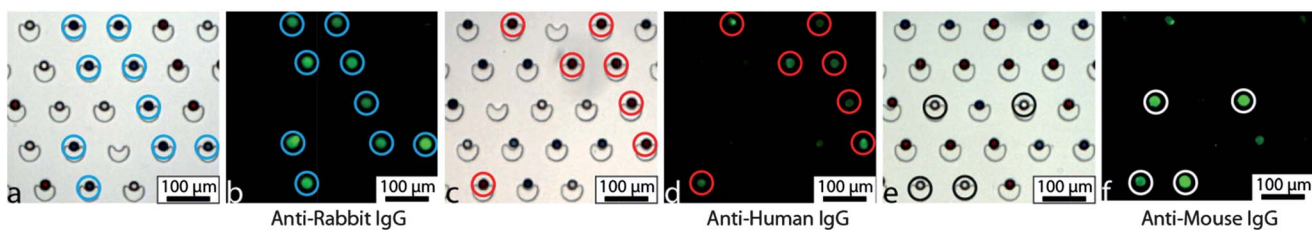


Fig. 6 Image sequence of a multiplexed immunoassay using colored beads. In each case all beads have been exposed to one secondary IgG (anti-rabbit, anti-human and anti-mouse). a) and b) Beads exposed to anti-rabbit IgG which only attach to the beads coated with rabbit IgG (blue beads). c) and d) Analyte contains anti-human IgG which only attaches to beads coated with human IgG (red beads). e) and f) beads coated with mouse IgG (white) exposed to anti-mouse IgG.

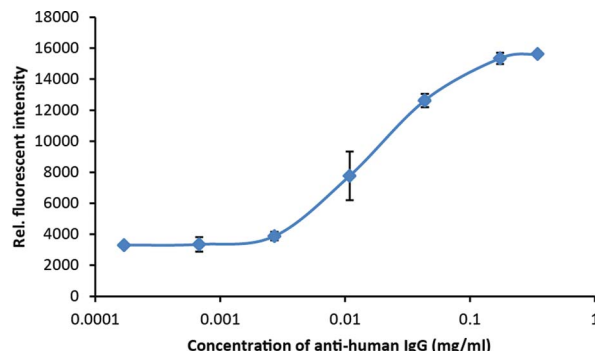


Fig. 7 Calibration curve for on-disc immunoassay for goat anti-human IgG.

a single focal plane, this platform is well suited for bead-based immunoassays with low-complexity instrumentation compared to complex, sheath-flow based commercial flow cytometers. In order to demonstrate this unique capability, a single-step antibody assay has been chosen. 20-μm polystyrene beads have been coated with antibodies and the assay has been performed according to the protocol described previously.

Fig. 6 represents the results of the assay, where the beads have been captured and subsequently exposed to an analyte solution containing one secondary antibody. The calibration curve obtained for the assay using beads coated with human IgG and anti-human Ab in the analyte is shown in Fig. 7. Due to the fact that the beads are individually located in a well-defined array within the same focal plane, readout of the assay is straight forward and multiplexing can easily be achieved by using beads of different colors corresponding to the surface-immobilized antibody. The main constraints are that the color of the beads is well distinguishable and that none of the dyes used to color the beads is auto fluorescent at the same wavelength as the fluorophore attached to the detection anti bodies.

With this approach only one fluorescent dye, *i.e.* only one light source and set of filters is needed for the detection and hence the cost for the readout instrument can be notably reduced.

Conclusion and outlook

In summary we presented a novel, centrifugal microfluidic platform for highly efficient trapping, distribution and treatment of beads using sedimentation under stagnant flow conditions. The experiments show that our platform is capable of very high

capture efficiencies (close to 100%) paired with a high array occupancy. The maximum as well as the width of the particle occupancy distribution are primarily governed by the ratio between the bead diameters and the characteristic length scale of the active capture site as well as the protocols of the rotational frequency. The here presented, arrayed alignment of individual particles in the same focal plane greatly facilitates detection and readout of signals from the particles. Furthermore, it assures homogeneous assay conditions across the entire bead population. We also demonstrated the capability of our novel platform to perform color-multiplexed, bead-based immunoassays. Future work will concentrate on applying these capabilities to clinically relevant, disease-specific test panels featuring multiplexed immunoassays with integrated sample preparation. Also cell detection and screening will be implemented.

Acknowledgements

This material is based upon works supported by the Science Foundation Ireland under Grant No. 10/CE/B1821 and the Irish Cancer Society Research Fellowship Award CRF10KIJ.

References

- 1 P. S. Dittrich and A. Manz, Lab-on-a-chip: microfluidics in drug discovery, *Nat. Rev. Drug Discovery*, 2006, **5**, 210–218.
- 2 J. Nilsson, M. Evans, B. Hammarstrom and T. Laurell, Review of cell and particle trapping in microfluidic systems, *Anal. Chim. Acta*, 2009, **649**, 141–157.
- 3 A. R. Wheeler, W. R. Thronset, R. J. Whelan, A. M. Leach, R. N. Zare, Y. H. Liao, K. Farrell, I. D. Manger and A. Daridon, Microfluidic device for single-cell analysis, *Anal. Chem.*, 2003, **75**, 3581–3586.
- 4 W. H. Tan and S. Takeuchi, A trap-and-release integrated microfluidic system for dynamic microarray applications, *Proc. Natl. Acad. Sci. U. S. A.*, 2007, **104**, 1146–1151.
- 5 S. Kobel, A. Valero, J. Latt, P. Renaud and M. Lutolf, Optimization of microfluidic single cell trapping for long-term on-chip culture *Lab Chip*, **10**, pp. 857–863.
- 6 M. Ikami, A. Kawakami, M. Kakuta, Y. Okamoto, N. Kaji, M. Tokeshi and Y. Baba, Immuno-pillar chip: a new platform for rapid and easy-to-use immunoassay *Lab on a Chip*, **10**, pp. 3335–3340.
- 7 L. Rieger, M. Grumann, T. Nann, J. Riegler, O. Ehrl, W. Bessler, K. Mittenbuehler, G. Urban, L. Pastewka, T. Brenner, R. Zengerle and J. Ducre, Read-out concepts for multiplexed bead-based fluorescence immunoassays on centrifugal microfluidic platforms, *Sens. Actuators, A*, 2006, **126**, 455–462.
- 8 R. D. Oleschuk, L. L. Shultz-Lockyear, Y. B. Ning and D. J. Harrison, Trapping of bead-based reagents within microfluidic systems: On-chip solid-phase extraction and electrochromatography, *Anal. Chem.*, 2000, **72**, 585–590.

- 9 M. Yang, C. Li and J. Yang, Cell Docking and On-Chip Monitoring of Cellular Reactions with a Controlled Concentration Gradient on a Microfluidic Device, *Anal. Chem.*, 2002, **74**, 3991–4001.
- 10 D. Di Carlo, L. Y. Wu and L. P. Lee, Dynamic single cell culture array, *Lab Chip*, 2006, **6**, 1445–1449.
- 11 A. M. Skelley, O. Kirak, H. Suh, R. Jaenisch and J. Voldman, Microfluidic control of cell pairing and fusion, *Nat. Methods*, 2009, **6**, 147–152.
- 12 M. Khouri, A. Bransky, N. Korin, L. C. Konak, G. Enikolopov, I. Tzchori and S. Levenberg, A microfluidic traps system supporting prolonged culture of human embryonic stem cells aggregates, *Biomed. Microdevices*, 2010, **12**, 1001–1008.
- 13 M. Kim, B. C. Isenberg, J. Sutin, A. Meller, J. Y. Wong and C. M. Klapperich, Programmed trapping of individual bacteria using micrometre-size sieves, *Lab Chip*, 2011, **11**, 1089–1095.
- 14 J. Y. Park, M. Morgan, A. N. Sachs, J. Samorezov, R. Teller, Y. Shen, K. J. Pienta and S. Takayama, Single cell trapping in larger microwells capable of supporting cell spreading and proliferation, *Microfluid. Nanofluid.*, 2010, **8**, 263–268.
- 15 J. R. Rettig and A. Folch, Large-Scale Single-Cell Trapping And Imaging Using Microwell Arrays, *Anal. Chem.*, 2005, **77**, 5628–5634.
- 16 S. Lee, J. Y. Kang, I. Lee, S. Ryu, S. Kwak, K. Shin, C. Kim, H. Jung and T. Kim, Single-cell assay on CD-like lab chip using centrifugal massive single-cell trap, *Sens. Actuators, A*, 2008, **143**, 64–69.
- 17 R. Martinez-Duarte, R. A. Gorkin III, K. Abi-Samra and M. J. Madou, The integration of 3D carbon-electrode dielectrophoresis on a CD-like centrifugal microfluidic platform, *Lab Chip*, 2010, **10**, 1030–1043.
- 18 M. Boettcher, M. S. Jaeger, L. Rieger, J. Ducrée, R. Zengerle and C. Duschl, Lab-on-chip-based cell separation by combining dielectrophoresis and centrifugation, *Biophys. Rev. Lett.*, 2006, **1**, 443–451.
- 19 J. Ducrée, S. Haeberle, S. Lutz, S. Pausch, F. von Stetten and R. Zengerle, The centrifugal microfluidic bio-disk platform, *J. Micromech. Microeng.*, 2007, **17**, S103–S115.
- 20 M. Madou, J. Zoval, G. Jia, H. Kido, J. Kim and N. Kim, Lab on a CD, *Annu. Rev. Biomed. Eng.*, 2006, **8**, 601–628.
- 21 R. Gorkin, J. Park, J. Siegrist, M. Amasia, B. S. Lee, J. Park, J. Kim, H. Kim, M. Madou and Y. Cho, Centrifugal microfluidics for biomedical applications, *Lab Chip*, 2010, **10**, 1758–1773.
- 22 L. Rieger, M. Grumann, J. Steigert, S. Lutz, C. P. Steinert, C. Mueller, J. Viertel, O. Prucker, J. Rühe, R. Zengerle and J. Ducrée, Single-step centrifugal hematocrit determination on a 10-\$ processing device, *Biomed. Microdevices*, 2007, **9**, 795–799.
- 23 T. Thorsen, S. J. Maerkl and S. R. Quake, Microfluidic Large-Scale Integration, *Science*, 2002, **298**, 580–584.
- 24 K. Hosokawa, K. Sato, N. Ichikawa and M. Maeda, Power-free poly(dimethylsiloxane) microfluidic devices for gold nanoparticle-based DNA analysis, *Lab Chip*, 2004, **4**, 181–185.
- 25 M. Grumann, T. Brenner, C. Beer, R. Zengerle and J. Ducrée, Visualization of flow patterning in high-speed centrifugal microfluidics, *Rev. Sci. Instrum.*, 2005, **76**, 25101–25101-6.